REVERSE ENGINEERING MODELING PROCESSING AND FABRICATION OF VORONOI PERFORATED ANKLE-FOOT ORTHOSIS

Zakki Fuadi Emzain[1]*, AM. Mufarrih[1], Moh Hartono[1], Nanang Qosim[1], Yusuf Dewantoro Herlambang[2]

[1] *Politeknik Negeri Malang, Department of Mechanical Engineering, Malang, Indonesia*
[2] *Politeknik Negeri Semarang, Department of Mechanical Engineering, Semarang, Indonesia*
* zfemzain@polinema.ac.id

The ankle may not function optimally because of an ankle foot injury due to torn ligaments or foot drop, a post-stroke effect of hemiplegia. One treatment that can be done for sufferers of ankle foot injury and foot drop is using an ankle foot orthosis (AFO). Reverse engineering (RE) and additive manufacturing (AM) technologies can be utilized within the medical domain, specifically for producing prosthetic devices and orthoses that include optimal fit, lightweight characteristics, and cost-effectiveness. This study aims to create an optimized design for an ankle-foot orthosis by utilizing reverse engineering techniques, followed by an analysis of its performance using finite element simulation. The research process involved several key steps, namely 3D Scanning, CAD modeling, model analysis, and 3D printing. The findings of the model study after the implementation of Voronoi ventilation holes indicated that the highest equivalent stress observed in the model, with a shell element thickness of 1.4 mm, amounted to 21.12 MPa. This result represented an elevation of 11.74% compared to the model before introducing Voronoi ventilation holes. Nevertheless, there was a reduction in the model's mass by 20.3%, specifically from an initial weight of 400.86 grams to a final weight of 319.51 grams. On the contrary, despite a fall in the safety factor, it continues to be considered safe, with a value of 2.84.

Keywords: additive manufacturing, ankle foot orthosis, finite element analysis, reverse engineering, Voronoi pattern

1 INTRODUCTION

The ankle is a vital anatomical structure within the human body that serves a crucial function in several everyday tasks, including standing, walking, running, and jumping. Nevertheless, the ankle's ideal functioning may be compromised as a result of an ankle foot injury caused by torn ligaments or foot drop, which is a post-stroke manifestation of hemiplegia [1, 2]. Traumatic prolonged injury to the ankle can also cause ankle osteoarthritis (AO) and lower extremity motor dysfunction [3]. One treatment that can be done for sufferers of ankle foot injury and foot drop is the wearing of an ankle foot orthosis (AFO). AFO functions to provide limiting torque in cases of muscle spasm and can provide additional torque for dorsiflexion and plantarflexion [4, 6]. The use of AFOs has been proven to effectively improve walking ability in stroke patients with gait disorders, prevent or correct ankle deformities, and maintain stability of lower leg joints [7]. Proper orthosis design can encourage the patient's rehabilitation process and restore normal gait [8, 9].

The development of ankle foot orthoses (AFOs) has been researched since the 1970s. Several types of AFOs include passive ankle-foot orthoses (PAFOs), passive non-articulating ankle-foot orthoses (PNAAFOs), semi-active ankle-foot orthoses (SAFOs), and active ankle-foot orthoses (AAFOs). PNAAFOs are generally made from thermoplastic or carbon composite, which is light but requires expert therapy to make it and in contact with the patient. Meanwhile, PAFOs and SAFOs can provide a little movement because they have features such as hinge, spring, oil damper, shape memory alloys, elastic actuator, magnetorheological fluid, and spring clutch. On the other hand, AAFOs are more sophisticated with pneumatic propulsion and hydraulic actuator/system/artificial muscle, which provides dynamic torque that can create flexion and dorsiflexion movements [10]. However, these devices are becoming heavier and an issue that has become the subject of recent research.

Additive manufacturing (AM) technology has been widely used, including in the medical industry, where it is cost-effective and can print geometrically complex objects [11, 12]. Examples of some applications are the manufacture of medicines, medical implants, and medical devices [13]. This technological advancement facilitates the development of a customized orthotic device that is tailored to the patient's specific anthropometric measurements [14]. One notable benefit of 3D printers is their inherent ease in creating models, facilitating the manufacturing process by enabling swift production. Moreover, the use of 3D printers can result in substantial cost savings, rendering them highly ideal for serving as a viable option in the creation of orthoses [15].

The utilization of ankle foot orthoses produced by 3D printers has been demonstrated to have a noteworthy impact as an alternative to traditional ankle foot orthoses, including those made from casts, thermoplastic materials, and braces. The subject in question exhibits promising potential for future development [16]. Numerous experts have conducted multiple prior investigations on advancing ankle-foot orthoses. Gautam Yadav and colleagues have simulated and analyzed an ankle foot orthosis (AFO) design that resembles the human foot by covering almost 75% of the foot surface. The material used is polypropylene with a thickness of 4 mm, which produces minor stress and is a good safety factor [17].

Journal of Applied Engineering Science

Vol. 22, No. 3, 2024

www.engineeringscience.rs

iipp publishing

Zakki Fuadi Emzain et al. - Reverse engineering modeling processing and fabrication of voronoi perforated ankle-foot orthosis

Falah Hasan Abdalsadah and colleagues have compared AFOs made traditionally with polypropylene and carbon fiber materials with additive manufacturing with PLA materials with several tests. The PLA-AFO design, which has regular hexagonal holes, produces minimum vibration after hammer and twist tests [18]. S F Khan and I Radzmi have researched an AFO design with specifications for height, length, and width of 300, 105, and 250 mm, sequentially designed manually and optimized. Of the three materials that were compared (polypropylene, HDPE, and PLA), the most suitable HDPE material was produced, has high flexibility and has sufficient resistance to deformation [19].

Prashanth R Kubasad and colleagues statically analyzed a passive AFO that they made with a combination of polypropylene and high-density polyethylene materials and two types of thicknesses of 3 mm and 4 mm. Using four running cycle variables as boundary conditions resulted in the conclusion that AFOs made from polypropylene and a thickness of 3 mm have good capabilities when receiving static forces [20]. Ratnesh Raj and his colleagues have tested an AFO design numerically and experimentally with variable PLA and PLA-C materials with an infill density of 100%. The results obtained are not much different from the two; the elastic energy, displacement, stress, and fracture location parameters are almost the same, with the conclusion that the 3D printer material PLA-C is stiffer than PLA [21].

Despite numerous research studies on the aforementioned static ankle foot orthoses, several prototype versions exhibit deficiencies. Several models are still manually designed without a 3D scanner, and several models containing full-solid materials have not yet been optimized for design. So, the prototype doesn't seem to fit the ankle's shape, making it less comfortable and too heavy to use. In the present context, specific ankle-foot orthoses exhibit a complex design and pose challenges in terms of usability [22, 23].

The availability of reverse engineering (RE) technology makes it feasible to produce 3D CAD models that are precise and comparable to the scanned surface, which is necessary to design an orthosis that fits well and conforms to the contours of the human body [24, 26]. This study aims to optimize the design of an ankle foot orthosis by utilizing reverse engineering modeling technology and analyzing it in finite element analysis before manufacturing it using additive manufacturing. Thus, this study's contribution is to optimize the design by applying the Voronoi pattern in the low-stress area to produce a prototype ankle-foot orthosis that better fits the shape of the ankle, is lighter, and can withstand stress.

2 METHODOLOGY

The present study encompassed four primary stages, namely 3D Scanning, CAD modeling, model analysis, and 3D Printing. Figure 1 illustrates a flowchart depicting the many steps of this investigation [27]. The initial stage was to scan the patient's feet and objects using a 3D scanner. The equipment prepared was a laptop, a 3D scanner device, and hand objects. The foot object had to remain still and not move during the scanning time for good scanning results. The position of the legs was able to be adjusted to hang like standing upright with the table as support. The 3D scanning device employed in this study was the EinScan Pro 2X Plus, which possesses well-suited specs for capturing detailed human body scans. This device offers four distinct scanning settings: Scan Modes, Scan Settings, Mesh Settings, and Mesh Processing. The configuration of the object scanning is depicted in Figure 2.
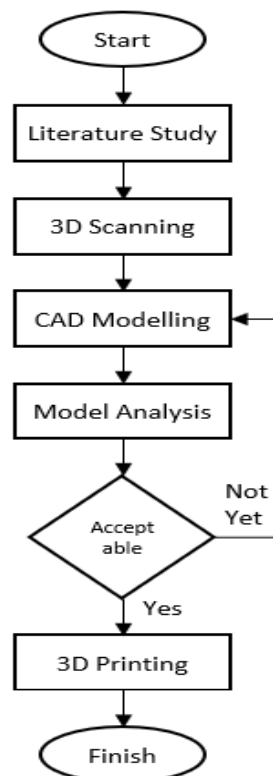

Fig. 1. Flowchart of research stages

Journal of Applied Engineering Science

Vol. 22, No. 3, 2024
www.engineeringscience.rs

iipp
publishing

Zakki Fuadi Emzain et al. - Reverse engineering modeling processing and fabrication of voronoi perforated ankle-foot orthosis
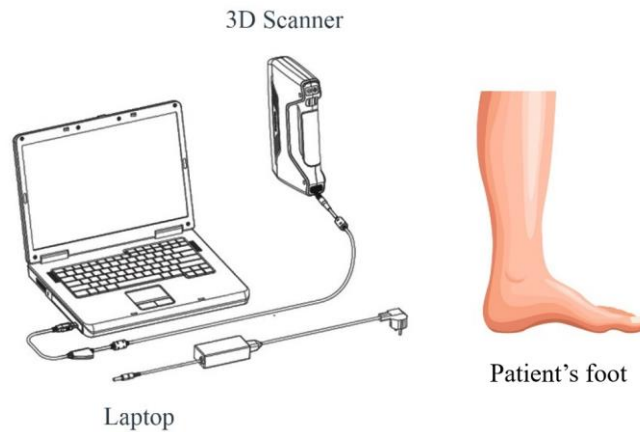
Fig. 2. Schematics of foot scanning

In the CAD modeling process, several core stages were carried out sequentially, namely model segmentation, model thickening, analysis pre-optimizing, making model ventilation holes, and making Velcro hook holes. Geomagic Design X, Autodesk Meshmixer, and Solidworks 2022 were the leading software used. The following procedures were undertaken to develop a design for the ankle-foot orthosis, encompassing the posterior aspect of the ankle-foot complex, extending from the distal portion of the calf to the distal end of the metatarsal region. The modeling design parameter can be illustrated in Figure 3, where h represents the height from the heel until below the calf, l represents the length alongside the sole, and w represents the width of half of the side foot surface. To optimize the design, a comparative analysis was performed before and after implementing the modification [28]. The analysis procedures were conducted to ascertain the magnitude of the maximal equivalent stress and identify the precise site at which this stress was experienced [29]. Additionally, the analysis model encompassed the analysis of the von Mises stress, elastic strain, and deformation outcomes. In addition, the analysis between before and after the holing model was compared.
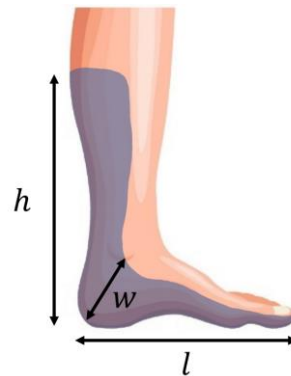

Fig. 3. Modeling design parameter

Subsequently, the perforated Ankle Foot Orthosis (AFO) model was manufactured using fused deposition modeling (FDM) 3D Printing technique as a means of prototyping. The FDM is one of the additive manufacturing techniques that has benefits for printing various materials, particularly polymer [30]. Polylactic Acid (PLA), the most often utilized plastic filament material, was employed as the principal substance. The choice of polylactic acid (PLA) as the preferable material is justified by its enhanced temperature resistance during extended printing operations, in contrast to acrylonitrile butadiene styrene (ABS) material, which is susceptible to warping [31]. Table 1 displays the mechanical properties of PLA material [27].

Table 1. Mechanical properties of the PLA

Characteristics	Value	Unit
Young's Modulus	3100	MPa
Density	1.24	g/cm^3
Yield Strength	60	MPa
Poisson's Ratio	0.39	

Journal of Applied Engineering Science

Vol. 22, No. 3, 2024

www.engineeringscience.rs

iipp
publishing

Zakki Fuadi Emzain et al. - Reverse engineering modeling processing and fabrication of voronoi perforated ankle-foot orthosis

3 RESULTS AND DISCUSSION

3.1 3D Scanning

The scanning process had four stages: Scan Modes, Scan Settings, Mesh Settings, and Mesh Processing. The area scanned started below the knees and ended at the tips of the toes. Some parameters include non-texture scan, hybrid alignment mode, lightning, 1 mm resolution, and watertight. The final results of object scanning of an adult male's feet are shown in Figure 4.

Fig. 4. The results of 3D Scanning

3.2 CAD Modelling

The segmentation step focused on the ankle area, including the calves, heels, and soles, creating a 3D mesh sketch line from the bottom of the calf to the tip of the metatarsal. The distance was approximately 1.5 to 2 cm, encircling around half of the back surface of the scanned foot. Then, the model design was created with a thin surface from the 3D mesh sketch path with 19 sketch chains using the Loft feature. Next, the model design was to extend the surface with adjustments similar to the insole to cover the entire sole. The next stage was to thicken the design surface to a thickness of 5 mm, and the edges of the design were smoothed with fillets of around 1 mm.

Before creating ventilation holes, the model design was briefly analyzed to find areas that experience high stress so that the holes will be made in areas with low stress. Voronoi perforations were implemented using a mesh reduction technique within regions with low stress levels. Subsequently, the dual edge functionality was used in the pattern type, utilizing element spacing of 0.2 mm and element dimension parameters of 5 mm. The final stage in CAD modeling was making holes for fastening straps such as Velcro. Three holes were created in three specific areas of the orthosis: the upper part of the calf, the middle of the heel, and the tip of the sole. These holes were present on both the right and left sides of the orthosis and had dimensions measuring 25 mm x 3 mm. Figure 5 shows the CAD modeling results of each stage.
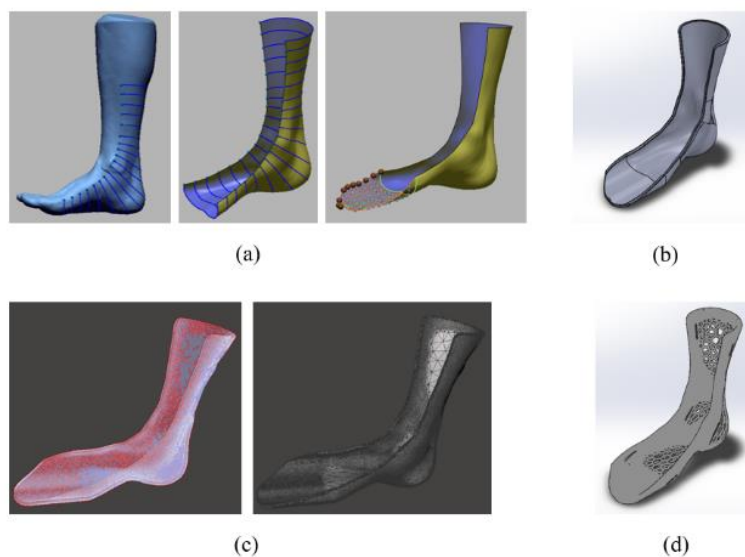

Fig. 5. The results of CAD Modelling (a) Segmentation, (b) Thickening, (c) Ventilation holes, (d) Velcro hook holes

3.3 Analysis Model

The first step involves manually performing the meshing process to generate elements with a predetermined element size of 5 mm. This element size was specifically chosen for the model before introducing a Voronoi hole, as it had

Journal of Applied Engineering Science

Vol. 22, No. 3, 2024

www.engineeringscience.rs

iipp
publishing

Zakki Fuadi Emzain et al. - Reverse engineering modeling processing and fabrication of voronoi perforated ankle-foot orthosis

been observed to yield a satisfactory mesh quality. The criteria for assessing the quality of meshing elements used the Skewness scale, where if the number of meshing elements was more significant on a scale range of 0 to 0.5, it was acceptable, and the closer to 0, the better the quality of the meshing elements. The element shapes used were QUAD4 – Quadrilateral (rectangle) with 4 Nodes and TRI3 – Triangle with 3 Nodes. This setting was chosen because the element's shape offered fast calculations and good stiffness accuracy. The analysis of the meshing outcomes revealed that a significant proportion of elements, encompassing both quad4 and tri3 types, had dimensions of 0.5 or less. This observation suggested that the elements possessed a relatively high level of quality. The meshing model results and meshing quality indicators are depicted in Figure 6.
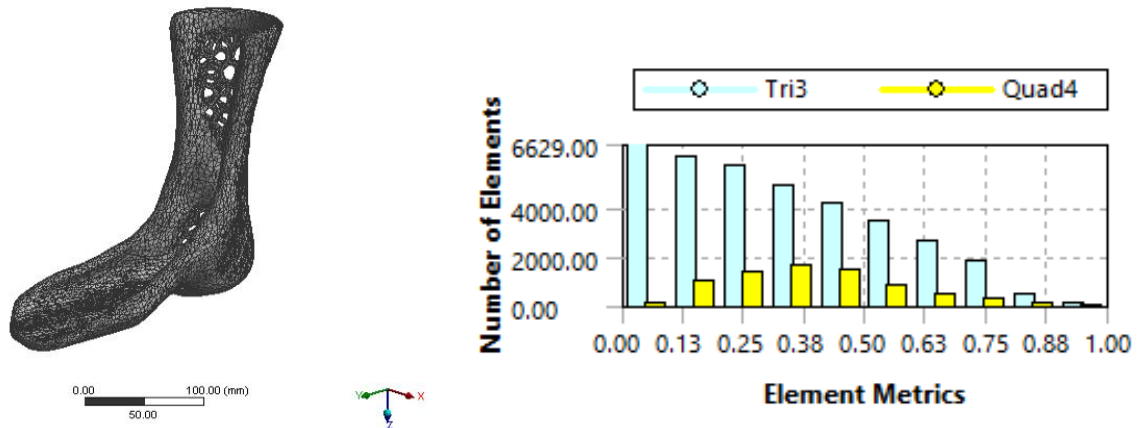

Fig. 6. Model meshing outcomes along with mesh quality markers

The boundary condition applied to the fixed support was located on the upper region of the model surface, namely spanning from the calf region to just before the heel region, excluding the Voronoi ventilation hole area, with the binding behind it. Meanwhile, the force was applied to the area of the sole as the center of force when the foot performed plantarflexion or dorsiflexion with a load ranging from 30 N to 240 N. The force interval in question represented the upper limit of force exerted when the model was utilized for immobilizing the patient's foot in a seated posture. The boundary conditions of the ankle foot orthosis model are illustrated in Figure 7.
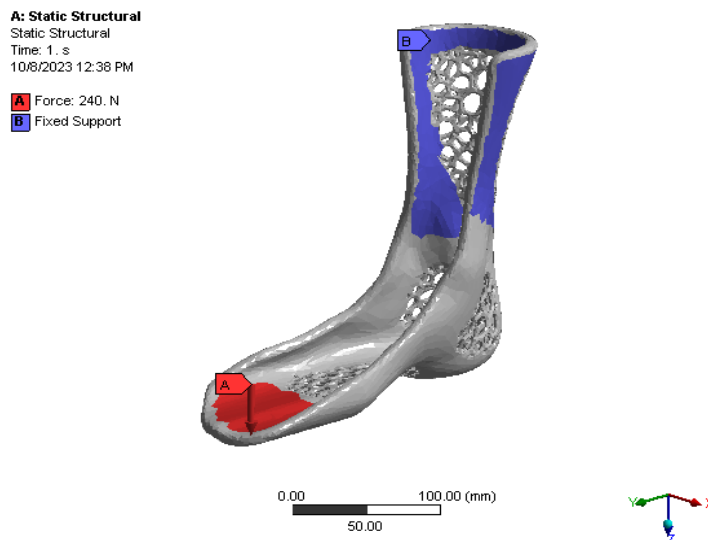

Fig. 7. Results of the boundary condition model

The analysis of the ankle foot orthosis model indicated that the highest stress levels were observed in the ankle arch region of the model, as determined by the equivalent (von Mises) stress aspect. This area was the central point of the model because the model was shaped like an elbow where the top end was like a fixed support area, and the other end was exposed to plantarflexion loading. So, this area naturally had the most significant stress. Furthermore, because the geometry model was included in the shell category, variations in the thickness of the shell element model could be adjusted. Variations in the thickness of shell elements that were regulated included thicknesses of 1.4 mm, 1.3 mm, 1.2 mm, and 1.1 mm. Figure 8 depicts the outcomes of comparable stress, highlighting the region of most tremendous stress and presenting a graphical representation of the correlation between load and stress across different thicknesses of the shell element model. From several types of thickness of shell element models, it could be assumed that the model had a maximum size of 1.4 mm and could withstand the most considerable load of 240 N and was still classified as safe for small structures with a maximum stress of 21.12 MPa. As mentioned above, the figure was deemed secure due to its significant disparity from the Tensile Strength value of the PLA material. The calculations utilizing the safety factor formula are outlined as follows.

$$n = \frac{\sigma_{yield}}{\sigma_{actual}}$$

(1)

Where n is the safety factor, σ_{yield} is the yield strength of the material, and σ_{actual} is the maximum stress that occurs, so the model had a safety factor of 2.84.
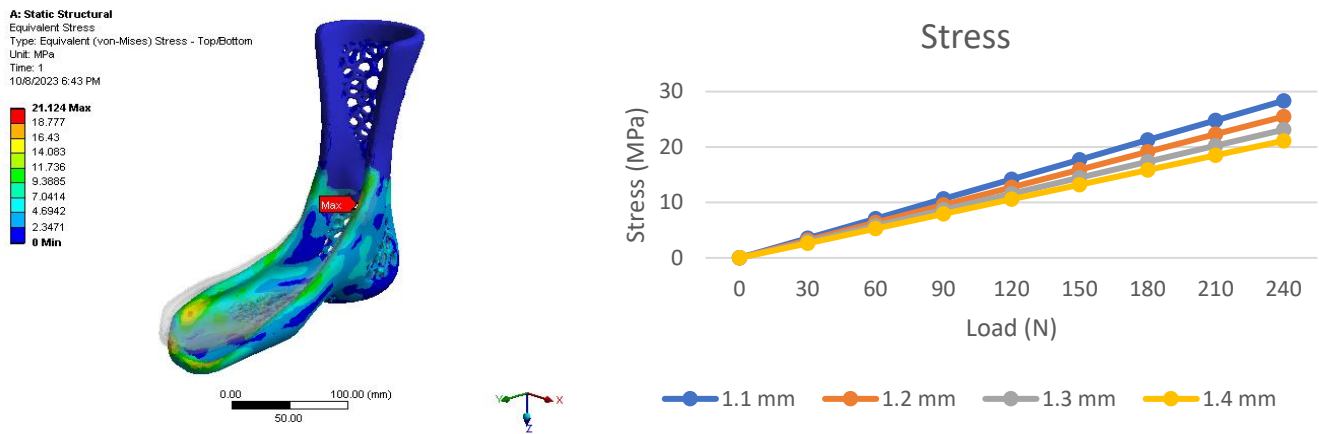

Fig. 8. Outcomes of the equivalent stress model and the load-stress graph derived from the shell element model with different thicknesses

In the meantime, the analysis outcomes about the ankle-foot orthosis model, specifically about the equivalent elastic strain aspect, exhibited a consistent pattern. Furthermore, the region with the highest strain coincided with the area of maximum stress equivalence. Among the three variations in model thickness, the shell element with a thickness of 1.1 mm exhibited the highest strain value at a significant load of 240 N, precisely measuring 0.011 mm. The strain value could be considered acceptable due to its comparatively tiny magnitude. In contrast, the model with a thickness of 1.4 mm exhibited a relatively lower maximum strain value of 0.008. Figure 9 illustrates the outcomes of the equivalent elastic strain, explicitly highlighting the region of maximal strain at the sole's tip. Additionally, it presents a graphical representation of the correlation between load and strain across different thicknesses of the shell element model.
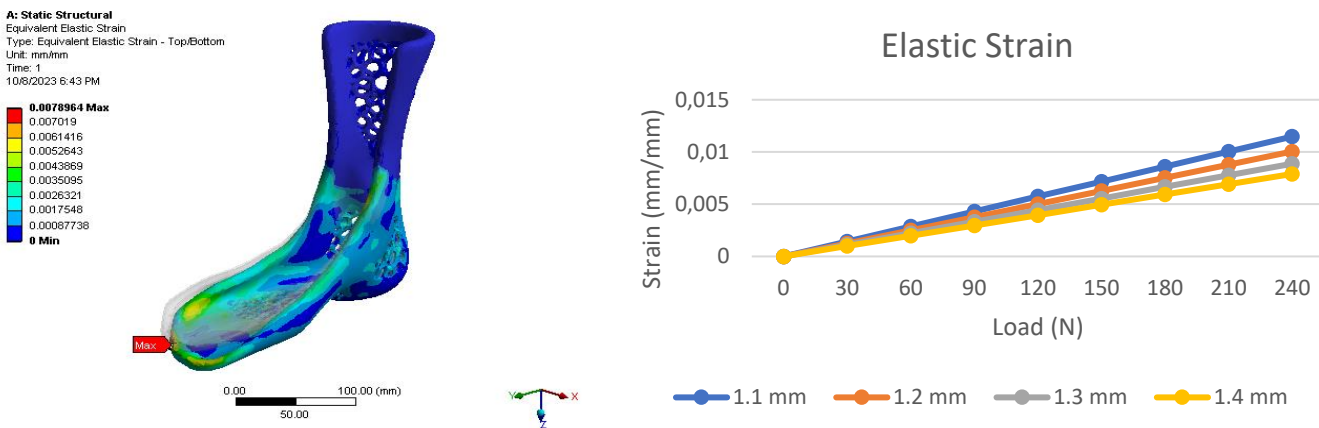

Fig. 9. Outcomes of the comparable elastic strain model and the load-strain graph derived from the shell element model with different thicknesses

Furthermore, the area near the tip of the model's foot had undergone the most distortion, according to the analysis of the ankle-foot orthosis model from the deformation perspective. This deformation was normal and could happen because this area was the core area that receives force when the sole experiences plantarflexion or dorsiflexion. The enormous deformation value occurred in the model with a thickness of shell element of 1.1 mm, namely 10.02 mm. By contrast, the model with a shell element thickness of 1.4 mm had the smallest deformation value, 6.82 mm. The deformation findings are displayed in Figure 10, along with a graph illustrating the relationship between load and deformation at different shell element model thicknesses and a maximum deformation area indication.

Journal of Applied Engineering Science

Vol. 22, No. 3, 2024

www.engineeringscience.rs

iipp
publishing

Zakki Fuadi Emzain et al. - Reverse engineering modeling processing and fabrication of voronoi perforated ankle-foot orthosis
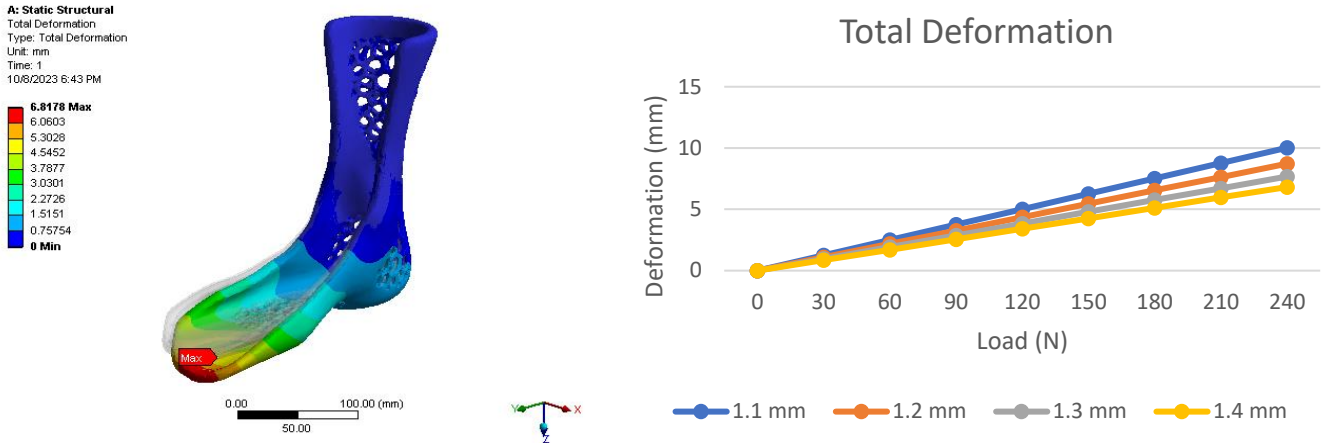
Fig. 10. Outcomes of the deformation model and the load-deformation graph derived from adjustments in the shell element model's thickness

From the analysis of the ankle foot orthosis, after the Voronoi ventilation holes were made above, a model with a shell element thickness of 1.4 mm was taken to compare with the model before the ankle foot orthosis was given the Voronoi ventilation holes. Table 2 comprehensively displays comparative statistics about mass, stress, deformation, and safety concerns.

Table 2. Mechanical properties of the PLA

Comparison	Before	After	%
Mass	400.86 g	319.51 g	-20.3
Stress	18.9 MPa	21.12 MPa	11.74
Deformation	6.05 mm	6.s82 mm	12.72
Safety Factor	3.17	2.84	-10.41

Table 2 above shows that adding Voronoi ventilation holes to the ankle-foot orthosis model reduced its mass by 20.3%. At the same time, the model's stress increased slightly by 11.74%. However, the safety factor remained relatively safe.

3.4 Model Fabrication

The ankle foot orthosis model was produced via the Creality CR 10S Pro 3D Printer, employing Polylactic Acid (PLA) filament material. The experimental setup involved the use of specific parameters, including a nozzle size of 0.4 mm, a layer height of 0.2 mm, a shell configuration of 0.8 mm, an infill density of 30%, a printing material temperature of 208 °C, and a print speed of 50 mm/s. The experimental outcomes demonstrated that the model was effectively fabricated with high quality. The produced model employed a thickness of 7 mm and exhibited a robust structure attributable to the high infill density, albeit leading to extended printing durations. The form of the model showed a high degree of physical fitness and provided a comfortable experience when worn.

To maintain a smooth inner surface, the general support was applied to the exterior surface of the model. Cleaning the preceding supports was imperative to get a polished appearance for the model. Following the completion of general support cleaning procedures, the measured weight of the model ankle foot orthosis was 340 grams. A discrepancy of 6.03% was observed when compared to the design. The model was expected to have significant efficacy in preserving muscular tone among individuals who had experienced a stroke and providing necessary support for the ankles and soles of the feet during foot rehabilitation fixation. The outcomes of the ankle foot orthosis's 3D print model are depicted in Figure 11 (a), while the application of the model on the foot is illustrated in Figure 11 (b).
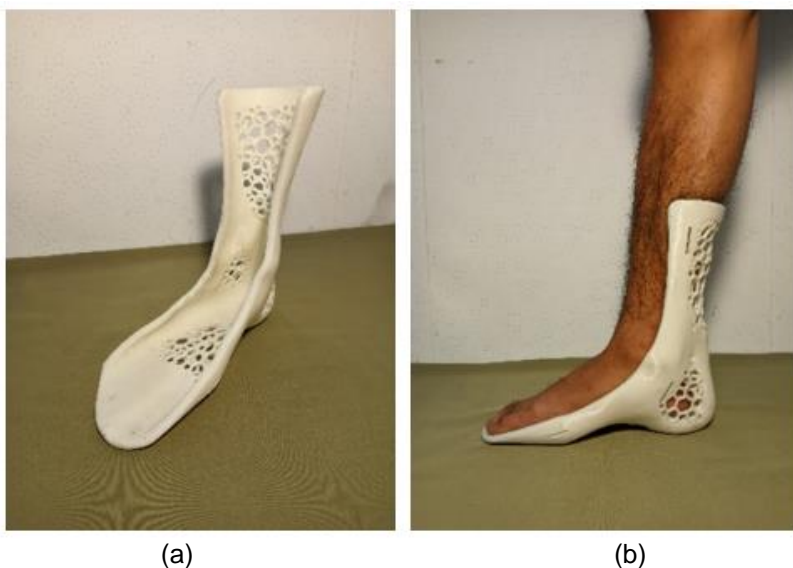
(a)　　　　　　　　(b)

Fig. 11. The results of model fabrication

4   CONCLUSIONS

Processing the reverse engineering technique of the Voronoi perforated ankle foot orthosis model's design was successfully optimized. This model resembled the human foot's instep from the calf to the tip. Manufacturing a model began with the object being scanned using a 3D scanner. Next, segmentation, thickening, stress simulation, design optimization through the creation of ventilation holes, and model format conversion were all done in 3D modeling. Before optimizing the creation of the Voronoi ventilation holes and comparing the two, the results of the model design optimization were next analyzed using the finite element method with variations in the thickness of the shell element and force with the same boundary conditions as the model.

The findings of the model study after implementing Voronoi ventilation holes indicate that the highest equivalent stress seen in the model, which had a shell element thickness of 1.4 mm, amounted to 21.12 MPa. This result represented an elevation of 11.74% compared to the model before introducing Voronoi ventilation holes. Nevertheless, the model's mass experienced a reduction of 20.3%, decreasing from an initial value of 400.86 grams to a final value of 319.51 grams. Despite a fall in the safety factor, it remained within an acceptable range, namely at a value of 2.84. The region exhibiting the highest level of comparable stress was observed in the anatomical region corresponding to the ankle arch in the model. This area was the central point of the model because the model was shaped like an elbow where the top end was like a fixed support area, and the other end was exposed to plantarflexion loading. A weight of 340 grams was successfully generated using 3D printing fabrication utilizing PLA material and FDM additive manufacturing type; this weight deviates 6.03% from the design.

5   ACKNOWLEDGEMENT

6   REFERENCES

[1] Pourhoseingholi, E., Saeedi, H., (2021). Role of the newly designed Ankle Foot Orthosis on balance related parametersin drop foot post stroke patients, J. Bodyw. Mov. Ther., vol. 26, p. 501–504, DOI: 10.1016/j.jbmt.2020.11.022

[2] Choo, Y. J., Chang, M. C., (2021). Commonly used types and recent development of ankle-foot orthosis: A narrative review, Healthcare, vol. 9, no. 8, p. 1-11, DOI: 10.3390/healthcare9081046

[3] Chung, C. L., DIangelo, D. J., Powell, D. W., Paquette, M. R., (2020). Biomechanical comparison of a new dynamic ankle orthosis to a standard ankle-foot orthosis during walking, J. Biomech. Eng., vol. 142, no. 5, p. 1-7, DOI: 10.1115/1.4045549

[4] Totah, D., Menon, M., Hershinow, C. J., Barton, K., Gates, D. H., (2019). The impact of ankle-foot orthosis stiffness on gait: a systematic literature review, Gait & Posture, vol. 69, p. 101–111, DOI: 10.1016/j.gaitpost.2019.01.020

[5] Chen, B., Zi, B., Zeng, Y., Qin, L., Liao, W. H., (2018). Ankle-foot orthoses for rehabilitation and reducing metabolic cost of walking: Possibilities and challenges. Mechatronics, vol. 53, p. 241–250. DOI: 10.1016/j.mechatronics.2018.06.014

[6] Vasiliauskaite, E., Ielapi, A., De Beule, M., Van Paepegem, W., Deckers, J. P., Vermandel, M., Forward, M., Plasschaert, F., (2019). A study on the efficacy of AFO stiffness prescriptions, Disabil. Rehabil. Assist. Technol., vol. 16, no. 1., p. 27-39, DOI: 10.1080/17483107.2019.1629114

Journal of Applied Engineering Science

Vol. 22, No. 3, 2024

www.engineeringscience.rs

iipp publishing

Zakki Fuadi Emzain et al. - Reverse engineering modeling processing and fabrication of voronoi perforated ankle-foot orthosis

[7] Choo, Y. J., Chang, M. C., (2021). Effectiveness of an ankle–foot orthosis on walking in patients with stroke: A systematic review and meta-analysis, Sci. Rep., vol. 11, no. 1, p. 1–12, DOI: 10.1038/s41598-021-95449-x

[8] Ielapi, A., Forward, M., De Beule, M., (2019). Computational and experimental evaluation of the mechanical properties of ankle foot orthoses: a literature review, Prosthet. Orthot. Int., vol. 43, no. 3, p. 339–348, DOI: 10.1177/0309364618824452

[9] Cárdenas, S. L. C., Guzmán A. A. L., Bautista J. A. R., Zavala A. H., (2018). A review in gait rehabilitation devices and applied control techniques. Disabil Rehabil Assist Technol., vol. 13, no. 8, p. 819–834, DOI: 10.1080/17483107.2018.1447611

[10] Zhou, C., Yang, Z., Li, K., Ye, X., (2022). Research and Development of Ankle–Foot Orthoses: A Review, Sensors, vol. 22, no. 17, p. 1-15, DOI: 10.3390/s22176596

[11] Li, C., Pisignano, D., Zhao, Y., Xue J., (2020). Advances in medical applications of additive manufacturing, Engineering, vol. 6, no. 11, p. 1222–1231, DOI: 10.1007/978-3-030-35876-1_6

[12] Kumar. R., Kumar, M., Chohan, J.S., (2021). The role of additive manufacturing for biomedical applications: A critical review. J Manuf Process, vol. 4, p. 828–850, DOI: 10.1016/j.jmapro.2021.02.022

[13] Young, K. J., Pierce, J. E., Zuniga, J. M., (2019). Assessment of body-powered 3D printed partial finger prostheses: a case study, 3D Print. Med., vol. 5, no. 1, p. 1–8, DOI: 10.1007/978-3-030-35876-1_6

[14] Choi, H., Seo, A., Lee, J., (2019). Mallet Finger Lattice Casts Using 3D Printing, J. Healthc. Eng., vol. 2019, p. 1-5, DOI: 10.1155/2019/4765043

[15] Zheng, Y., Liu, G., Yu, L., Wang, Y., Fang, Y., Shen, Y., Huang, X., Qiao, L., Yang, J., Zhang, Y., Hua, Z., (2020). Effects of a 3D-printed orthosis compared to a low-temperature thermoplastic plate orthosis on wrist flexor spasticity in chronic hemiparetic stroke patients: a randomized controlled trial, Clin. Rehabil., vol. 34, no. 2, p. 194–204, DOI: 10.1177/0269215519885174

[16] Rouf, S., Malik, A., Singh, N., Raina, A., Naveed, N., Siddiqui, M. I. H., Haq, M. I. U., (2022). Additive manufacturing technologies: Industrial and medical applications. Sustain Oper Comput., vol. 3, p. 258–274 DOI: 10.1016/j.susoc.2022.05.001

[17] Yadav G., Jain M.L., Gehlot V., (2021). Design and Analysis of Thermoplastic Polypropylene Ankle Foot Orthosis, J. Manuf. Eng., vol. 16, no. 3, p. 87–91, DOI: 10.37255/jme.v16i3pp087-091

[18] Abdalsadah, F. H., Hasan, F., Murtaza, Q., Khan, A. A., (2021). Design and manufacture of a custom ankle–foot orthoses using traditional manufacturing and fused deposition modeling, Prog. Addit. Manuf., vol. 6, no. 3, p. 555–570, DOI: 10.1007/s40964-021-00178-2

[19] Khan, S. F., Radzmi, I., (2021). Design and analysis of various thermoplastic for optimized ankle foot orthosis," J. Phys. Conf. Ser., vol. 2051, no. 1, p. 87–91, DOI: 10.1088/1742-6596/2051/1/012034

[20] Kubasad, P. R., Gawande, V. A., Todeti, S. R., Kamat, Y. D., Vamshi, N., (2020). Design and analysis of a passive ankle foot orthosis by using transient structural method, in Journal of Physics: Conference Series, 2020, vol. 1706, no. 1, p. 1-12, DOI: 10.1088/1742-6596/1706/1/012203

[21] Raj, R., Dixit, A. R., Łukaszewski, K., Wichniarek, R., Rybarczyk, J., Kuczko, W., Górski, F., (2022). Numerical and Experimental Mechanical Analysis of Additively Manufactured Ankle–Foot Orthoses, Materials (Basel)., vol. 15, no. 17, p. 1-15, DOI: 10.3390/ma15176130

[22] Sutton, L., Moein, H., Rafiee, A., Madden, J. D. W., Menon, C., (2016). Design of an assistive wrist orthosis using conductive nylon actuators, in 2016 6th IEEE International Conference on Biomedical Robotics and Biomechatronics (BioRob), 2016, p. 1074–1079, DOI: 10.1109/BIOROB.2016.7523774

[23] Ates, S., Mora-Moreno, I., Wessels, M., Stienen, A. H. A., (2015). Combined active wrist and hand orthosis for home use: Lessons learned, in 2015 IEEE International Conference on Rehabilitation Robotics (ICORR), 2015, p. 398–403, DOI: 10.1109/ICORR.2015.7281232

[24] Baglanis, A., (2022). Additive Manufacturing (AM) and Reverse Engineering (RE) in Orthopedic Applications: A Case Study in Total Elbow Arthroplasty (TEA). Dissertation, International Hellenic University, Greece.

[25] Anggoro, P. W., Tauviqirrahman, M., Jamari, J., Bayuseno, A. P., Bawono, B., Avelina, M.M., (2018). Computer-aided reverse engineering system in the design and production of orthotic insole shoes for patients with diabetes. Cogent Eng., vol. 5, no. 1, p. 1-20, DOI: 10.1080/23311916.2018.1470916

[26] Modi, Y. K., Khare, N., (2020). Patient-specific polyamide wrist splint using reverse engineering and selective laser sintering. Mater Technol., vol. 37, no. 2, p. 71–78, DOI: 10.1080/10667857.2020.1810926

[27] Emzain, Z. F., Qosim, N., Mufarrih, A. M., Hadi, S., (2022). Finite Element Analysis and Fabrication of Voronoi Perforated Wrist Hand Orthosis Based on Reverse Engineering Modelling Method, J. Appl. Eng. Technol. Sci., vol. 4, no. 1, p. 451–459, DOI: 10.37385/jaets.v4i1.1199

[28] Emzain, Z. F., Amrullah, U. S., Mufarrih, A., Qosim, N., Herlambang, Y. D., (2021). Design optimization of sleeve finger splint model using Finite Element Analysis, J. Polimesin, vol. 19, no. 2, p. 147–152, DOI: 10.30811/jpl.v19i2.2272

[29] Qosim, N., Monasari, R., Emzain, Z. F., Hakim, L., Sai'in, A., (2020). Finite Element Analysis of Miniplate for Post-Fracture Finger Rehabilitation Device, J Appl Eng Technol Sci., vol. 2, no. 1, p. 21–26, DOI: 10.37385/jaets.v2i1.160

[30] Mazzanti, V., Malagutti, L., Mollica, F., (2019). FDM 3D printing of polymers containing natural fillers: A review of their mechanical properties, Polymers (Basel)., vol. 11, no. 7, p. 1-22, DOI: 10.3390/polym11071094

[31] Yang, Y. S., Emzain, Z. F., Huang, S. C., (2021). Biomechanical Evaluation of Dynamic Splint Based on Pulley Rotation Design for Management of Hand Spasticity, IEEE Trans. Neural Syst. Rehabil. Eng., vol. 29, p. 683–689, DOI: 10.1109/TNSRE.2021.3068453